Supplementary material for:

Evolution of Non-Metallic Inclusions Through Processing in Ti-V Microalloyed 316L and Al-V Microalloyed 17-4PH Stainless Steels for Hipping Applications

María J. Balart[1*], Xinjiang Hao[1,2], Samuel Marks[1,3], Geoff D. West[1], Marc Walker[4] and Claire L. Davis[1]

[1]University of Warwick, WMG – Advanced Manufacturing and Materials Centre (AMMC), Coventry, CV4 7AL, UK
[2]Liberty Powder Metals, Materials Processing Institute, Eston Road, Middlesbrough, TS6 6US, UK
[3]Oxford Instruments NanoAnalysis, High Wycombe, Buckinghamshire, HP12 3SE, UK
[4]University of Warwick, Department of Physics, Gibbet Hill Road, Coventry, CV4 7AL, UK
[*]Corresponding author's present address: BCAST, Brunel University London, Uxbridge, Middlesex, UB8 3PH, UK

Emails: Maria.Balart@brunel.ac.uk; Xinjiang.Hao@libertypowdermetals.com; Sam.MARKS@oxinst.com; G.West@warwick.ac.uk; M.Walker@warwick.ac.uk; Claire.Davis@warwick.ac.uk

(a)

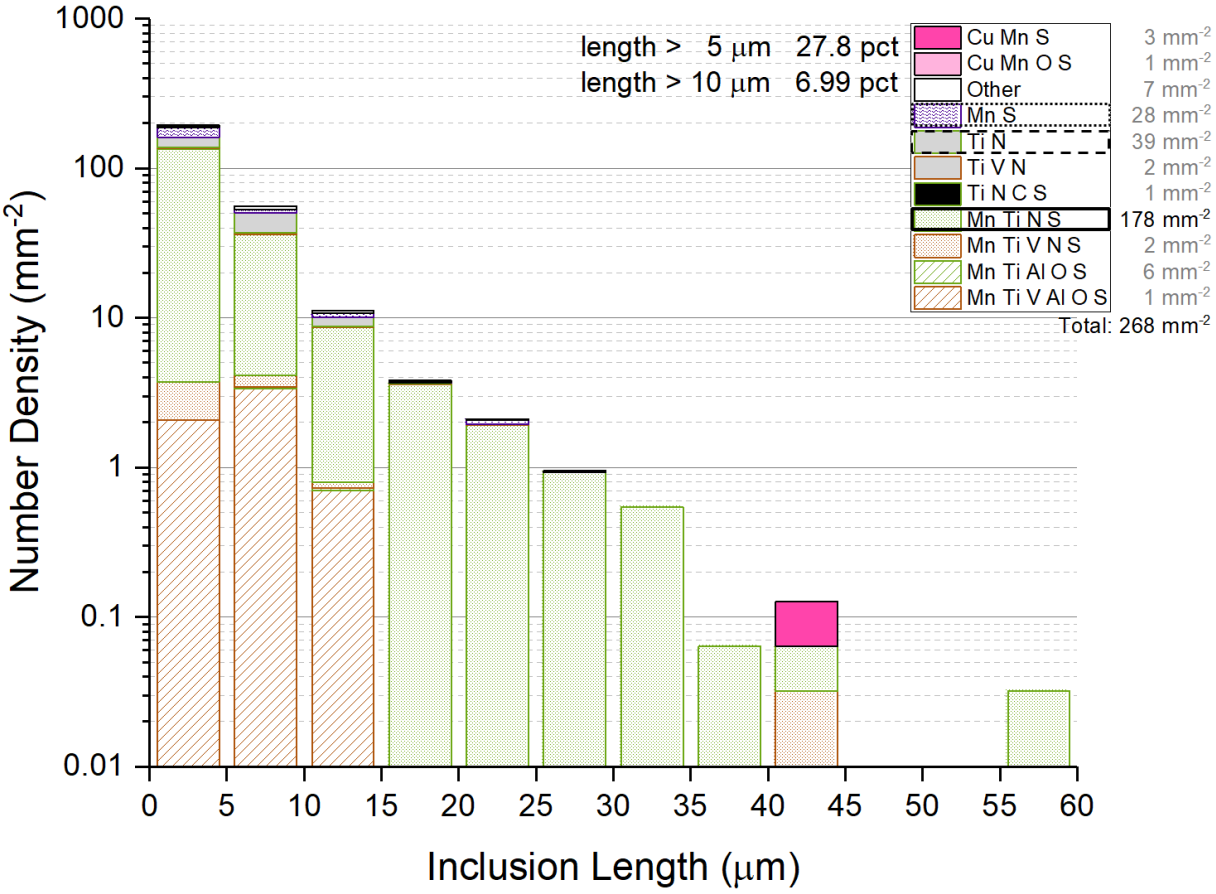
length > 5 μm 27.8 pct
length > 10 μm 6.99 pct
Cu Mn S 3 mm-2
Cu Mn O S 1 mm-2
Other 7 mm-2
Mn S 28 mm-2
Ti N 39 mm-2
Ti V N 2 mm-2
Ti N C S 1 mm-2
Mn Ti N S 178 mm-2
Mn Ti V N S 2 mm-2
Mn Ti Al O S 6 mm-2
Mn Ti V Al O S 1 mm-2
Total: 268 mm-2
Number Density (mm-2)
1000
100
10
1
0.1
0.01
0 5 10 15 20 25 30 35 40 45 50 55 60
Inclusion Length (μm)

(b)

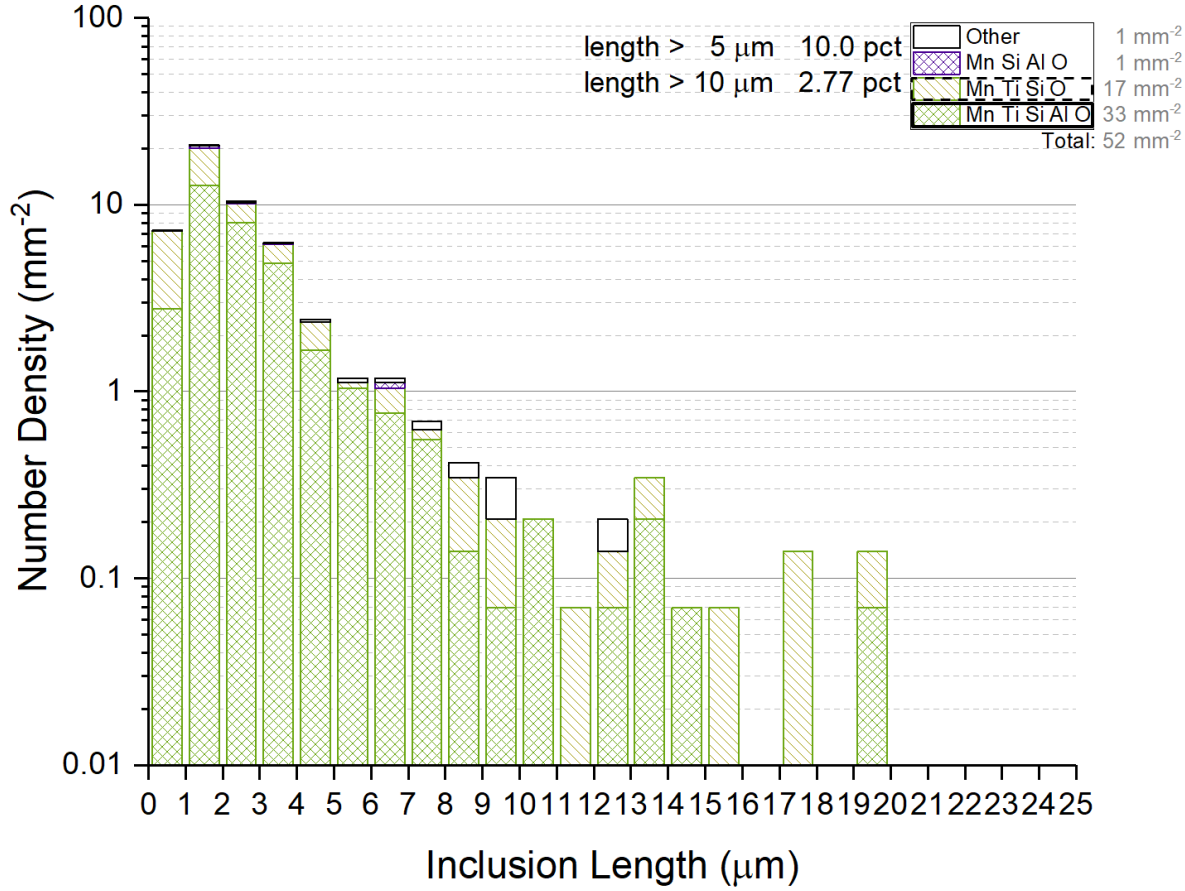
length > 5 μm 10.0 pct
length > 10 μm 2.77 pct
Other 1 mm-2
Mn Si Al O 1 mm-2
Mn Ti Si O 17 mm-2
Mn Ti Si Al O 33 mm-2
Total: 52 mm-2
Number Density (mm-2)
100
10
1
0.1
0.01
0 1 2 3 4 5 6 7 8 9 10 11 12 13 14 15 16 17 18 19 20 21 22 23 24 25
Inclusion Length (μm)

(c)

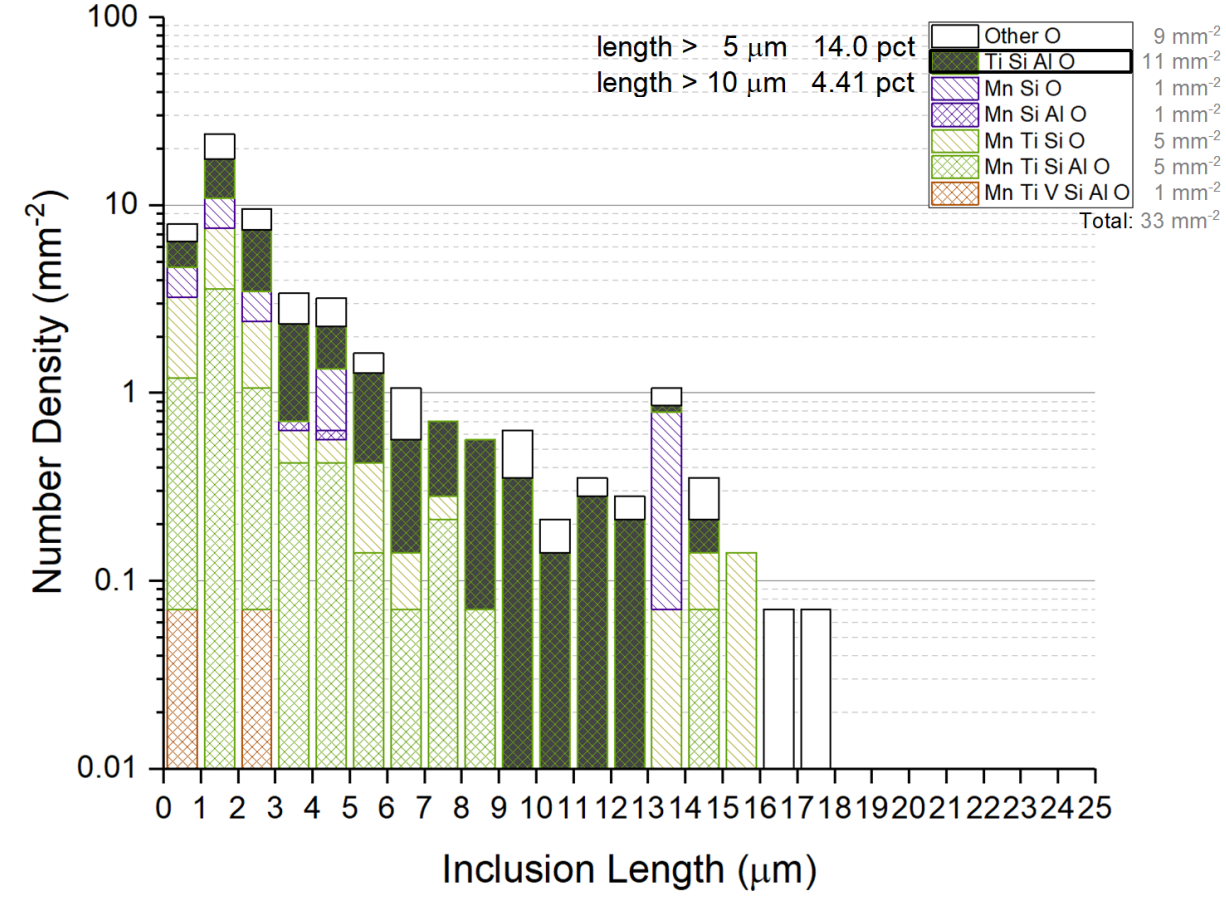
length > 5 μm 14.0 pct
length > 10 μm 4.41 pct
Other O 9 mm-2
Ti Si Al O 11 mm-2
Mn Si O 1 mm-2
Mn Si Al O 1 mm-2
Mn Ti Si O 5 mm-2
Mn Ti Si Al O 5 mm-2
Mn Ti V Si Al O 1 mm-2
Total: 33 mm-2
Number Density (mm-2)
Inclusion Length (μm)

(d)

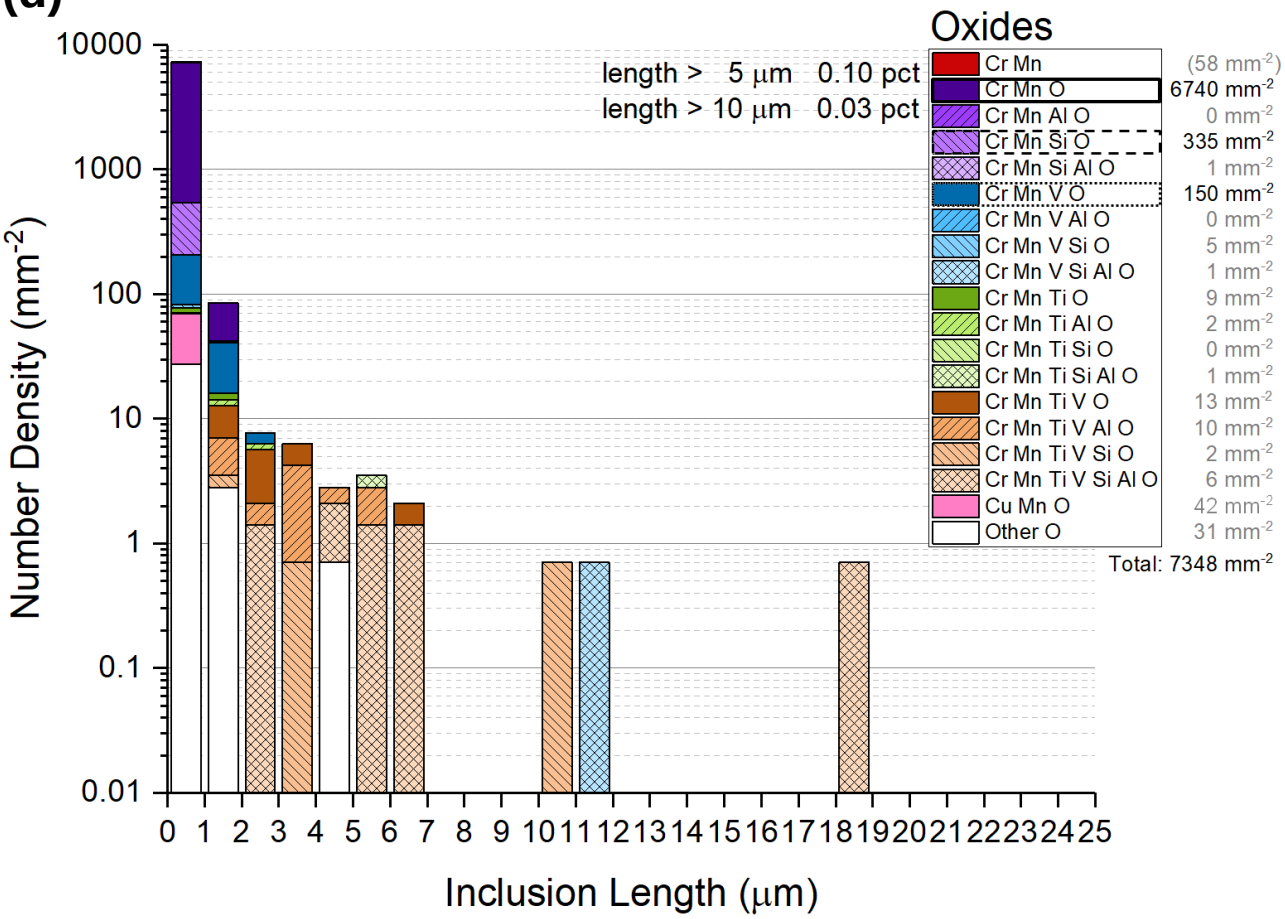
Oxides
length > 5 μm 0.10 pct
length > 10 μm 0.03 pct
Cr Mn (58 mm-2)
Cr Mn O 6740 mm-2
Cr Mn Al O 0 mm-2
Cr Mn Si O 335 mm-2
Cr Mn Si Al O 1 mm-2
Cr Mn V O 150 mm-2
Cr Mn V Al O 0 mm-2
Cr Mn V Si O 5 mm-2
Cr Mn V Si Al O 1 mm-2
Cr Mn Ti O 9 mm-2
Cr Mn Ti Al O 2 mm-2
Cr Mn Ti Si O 0 mm-2
Cr Mn Ti Si Al O 1 mm-2
Cr Mn Ti V O 13 mm-2
Cr Mn Ti V Al O 10 mm-2
Cr Mn Ti V Si O 2 mm-2
Cr Mn Ti V Si Al O 6 mm-2
Cu Mn O 42 mm-2
Other O 31 mm-2
Total: 7348 mm-2
Number Density (mm-2)
Inclusion Length (μm)

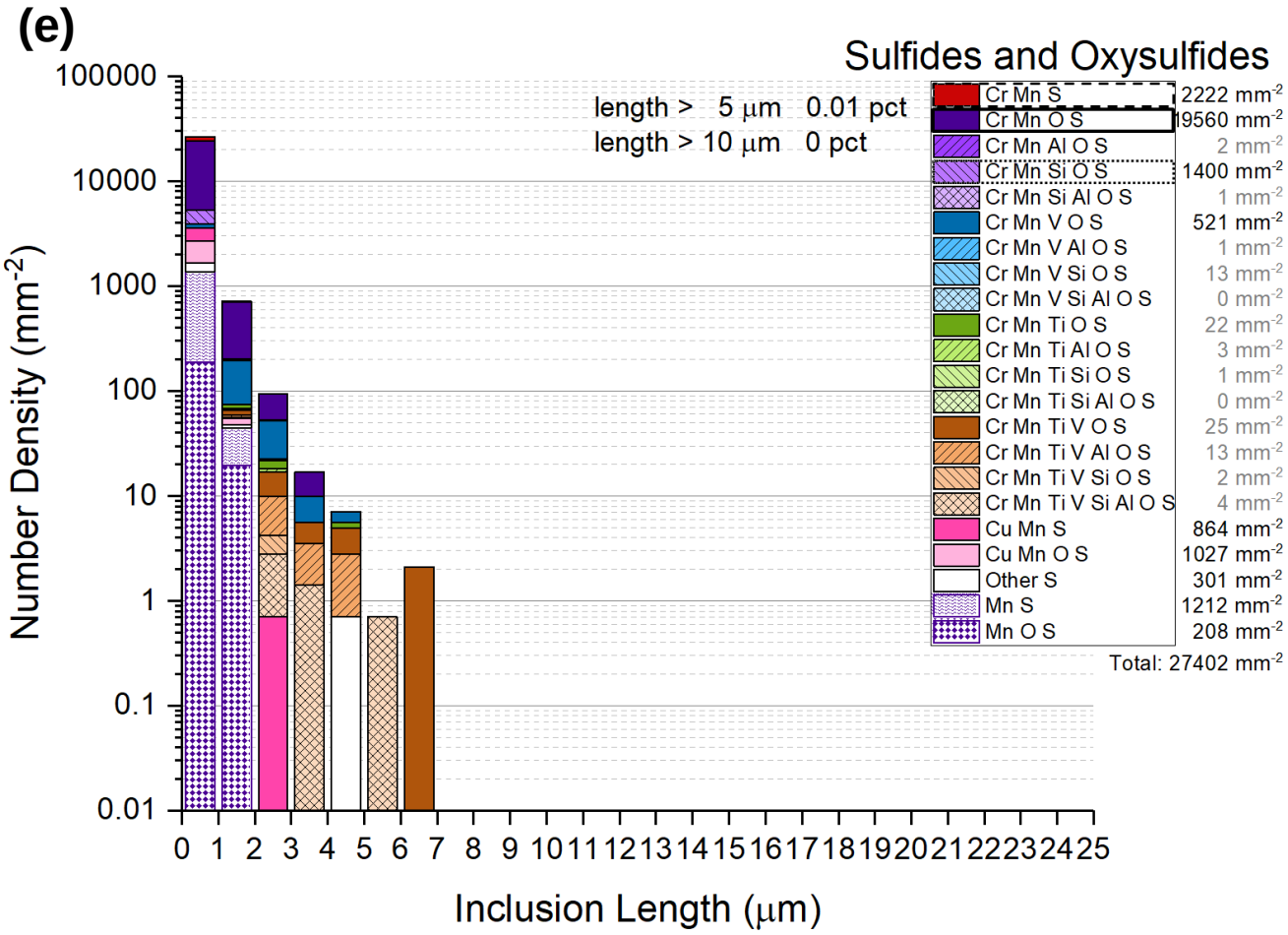
(e)
Sulfides and Oxysulfides
length > 5 μm 0.01 pct
length > 10 μm 0 pct
Cr Mn S 2222 mm-2
Cr Mn O S 19560 mm-2
Cr Mn Al O S 2 mm-2
Cr Mn Si O S 1400 mm-2
Cr Mn Si Al O S 1 mm-2
Cr Mn V O S 521 mm-2
Cr Mn V Al O S 1 mm-2
Cr Mn V Si O S 13 mm-2
Cr Mn V Si Al O S 0 mm-2
Cr Mn Ti O S 22 mm-2
Cr Mn Ti Al O S 3 mm-2
Cr Mn Ti Si O S 1 mm-2
Cr Mn Ti Si Al O S 0 mm-2
Cr Mn Ti V O S 25 mm-2
Cr Mn Ti V Al O S 13 mm-2
Cr Mn Ti V Si O S 2 mm-2
Cr Mn Ti V Si Al O S 4 mm-2
Cu Mn S 864 mm-2
Cu Mn O S 1027 mm-2
Other S 301 mm-2
Mn S 1212 mm-2
Mn O S 208 mm-2
Total: 27402 mm-2
Number Density (mm-2)
100000
10000
1000
100
10
1
0.1
0.01
0 1 2 3 4 5 6 7 8 9 10 11 12 13 14 15 16 17 18 19 20 21 22 23 24 25
Inclusion Length (μm)

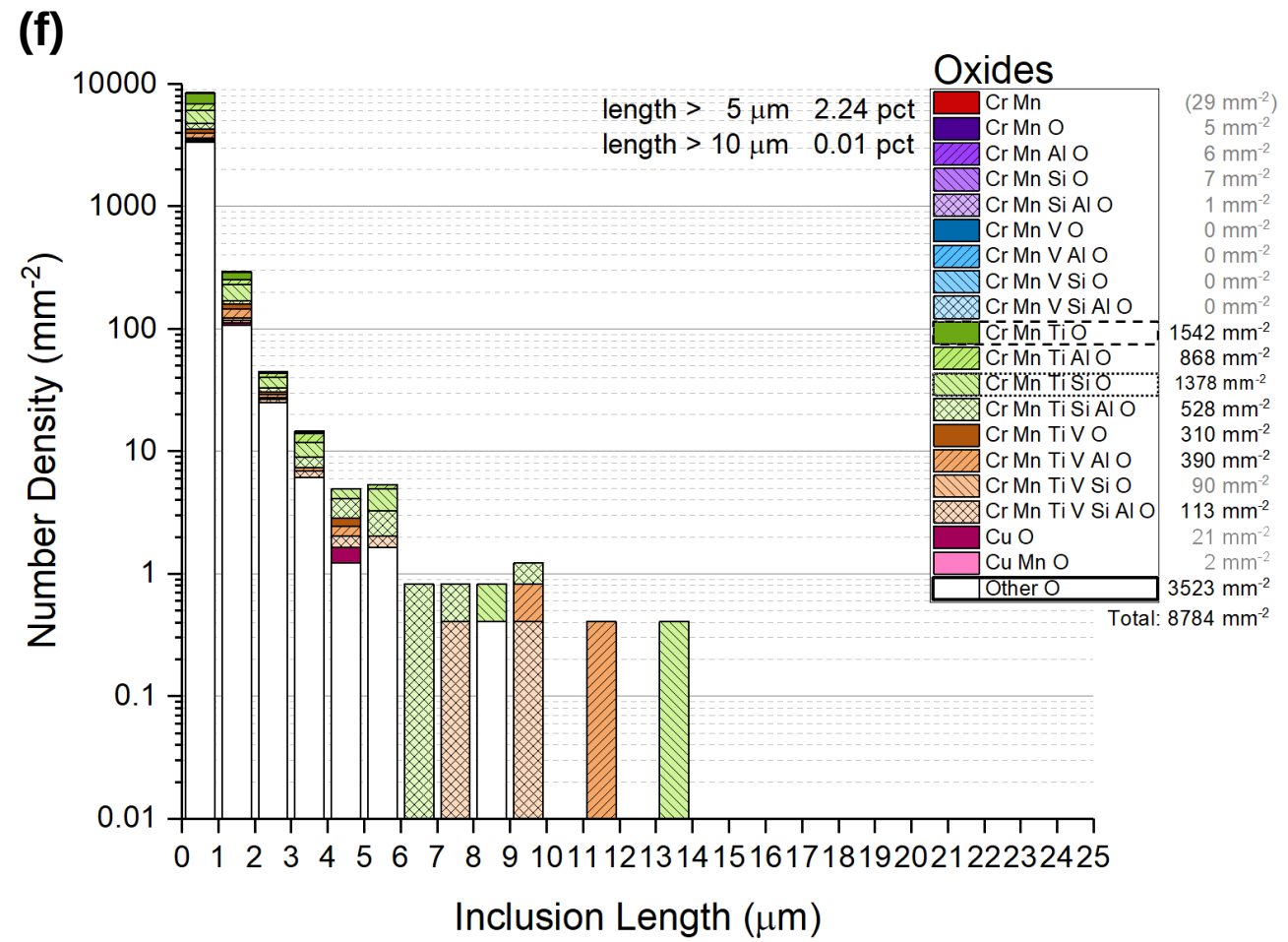
(f)
Oxides
length > 5 μm 2.24 pct
length > 10 μm 0.01 pct
Cr Mn (29 mm-2)
Cr Mn O 5 mm-2
Cr Mn Al O 6 mm-2
Cr Mn Si O 7 mm-2
Cr Mn Si Al O 1 mm-2
Cr Mn V O 0 mm-2
Cr Mn V Al O 0 mm-2
Cr Mn V Si O 0 mm-2
Cr Mn V Si Al O 0 mm-2
Cr Mn Ti O 1542 mm-2
Cr Mn Ti Al O 868 mm-2
Cr Mn Ti Si O 1378 mm-2
Cr Mn Ti Si Al O 528 mm-2
Cr Mn Ti V O 310 mm-2
Cr Mn Ti V Al O 390 mm-2
Cr Mn Ti V Si O 90 mm-2
Cr Mn Ti V Si Al O 113 mm-2
Cu O 21 mm-2
Cu Mn O 2 mm-2
Other O 3523 mm-2
Total: 8784 mm-2
Number Density (mm-2)
10000
1000
100
10
1
0.1
0.01
0 1 2 3 4 5 6 7 8 9 10 11 12 13 14 15 16 17 18 19 20 21 22 23 24 25
Inclusion Length (μm)

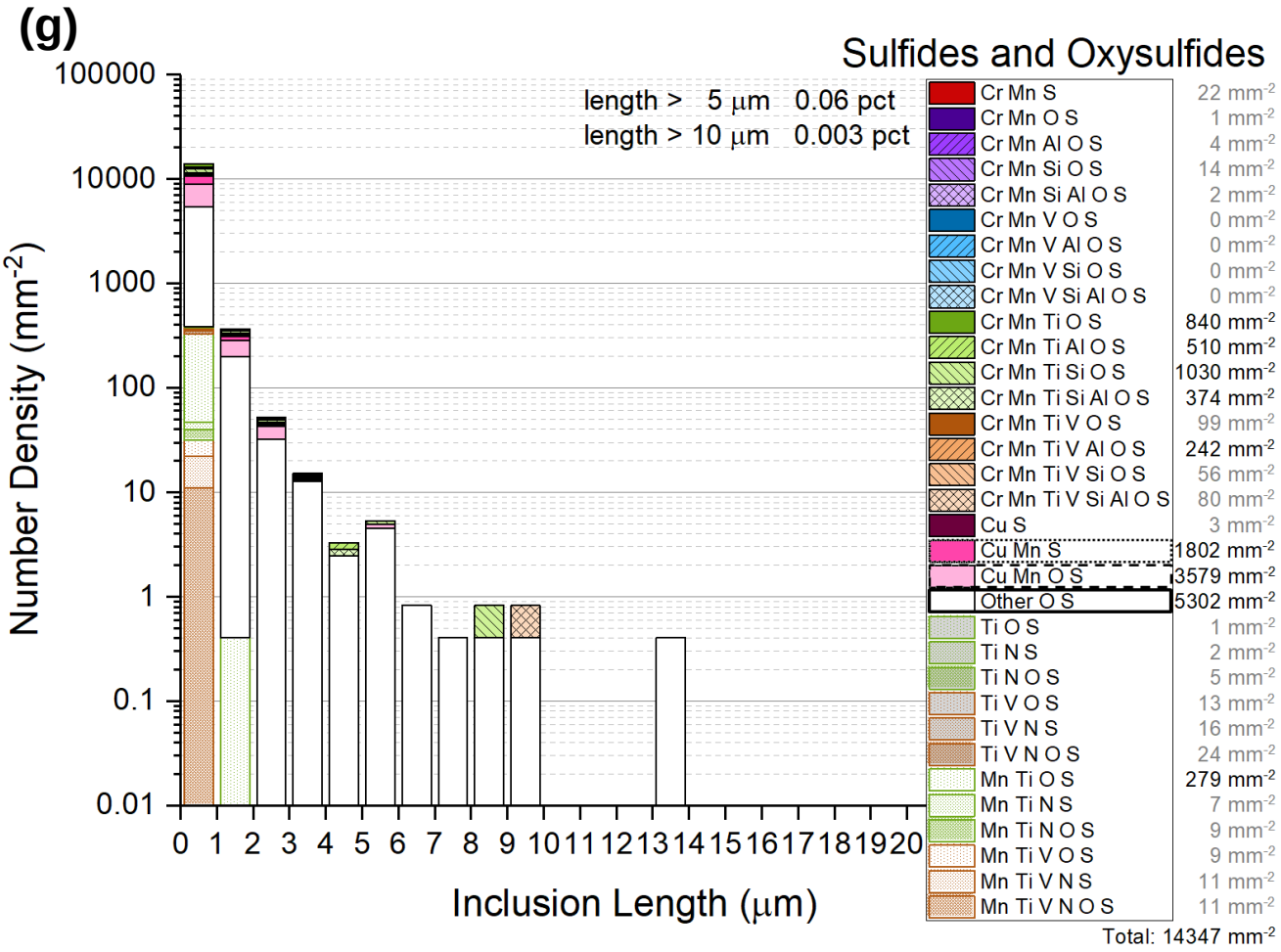

Fig. S-1 – Histograms of number density of non-metallic inclusions for the 316L stainless steel: (*a*) feedstock; (*b*) AMGA powder < 150 μm; (*c*) VIGA powder 106 to 150 μm; (*d*) and (*e*) AMGA HIP'd < 150 μm; and (*f*) and (*g*) VIGA HIP'd 106 to 150 μm samples. The top three categories are marked in descending order of their value by continuous, dashed and dotted boxes, respectively. Number density values less than 100 mm^{-2} have been marked in grey color. Note that Si- and Al-containing inclusions are marked with fill patterns: hatched towards the left denotes Si, hatched towards the right denotes Al and hatched towards both the left and the right denotes Si and Al.

(a)

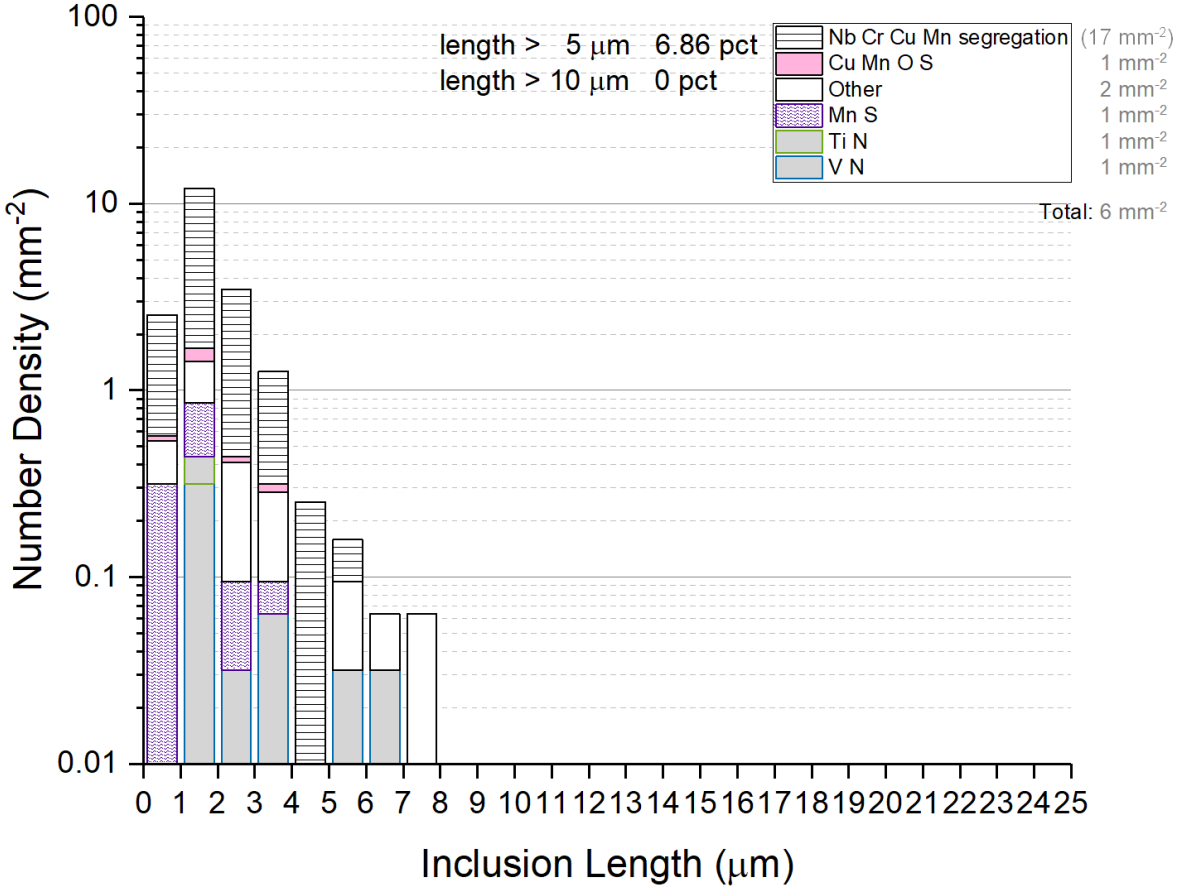
length > 5 μm 6.86 pct
length > 10 μm 0 pct
Nb Cr Cu Mn segregation (17 mm-2)
Cu Mn O S 1 mm-2
Other 2 mm-2
Mn S 1 mm-2
Ti N 1 mm-2
V N 1 mm-2
Total: 6 mm-2
Number Density (mm-2)
100
10
1
0.1
0.01
0 1 2 3 4 5 6 7 8 9 10 11 12 13 14 15 16 17 18 19 20 21 22 23 24 25
Inclusion Length (μm)

(b)

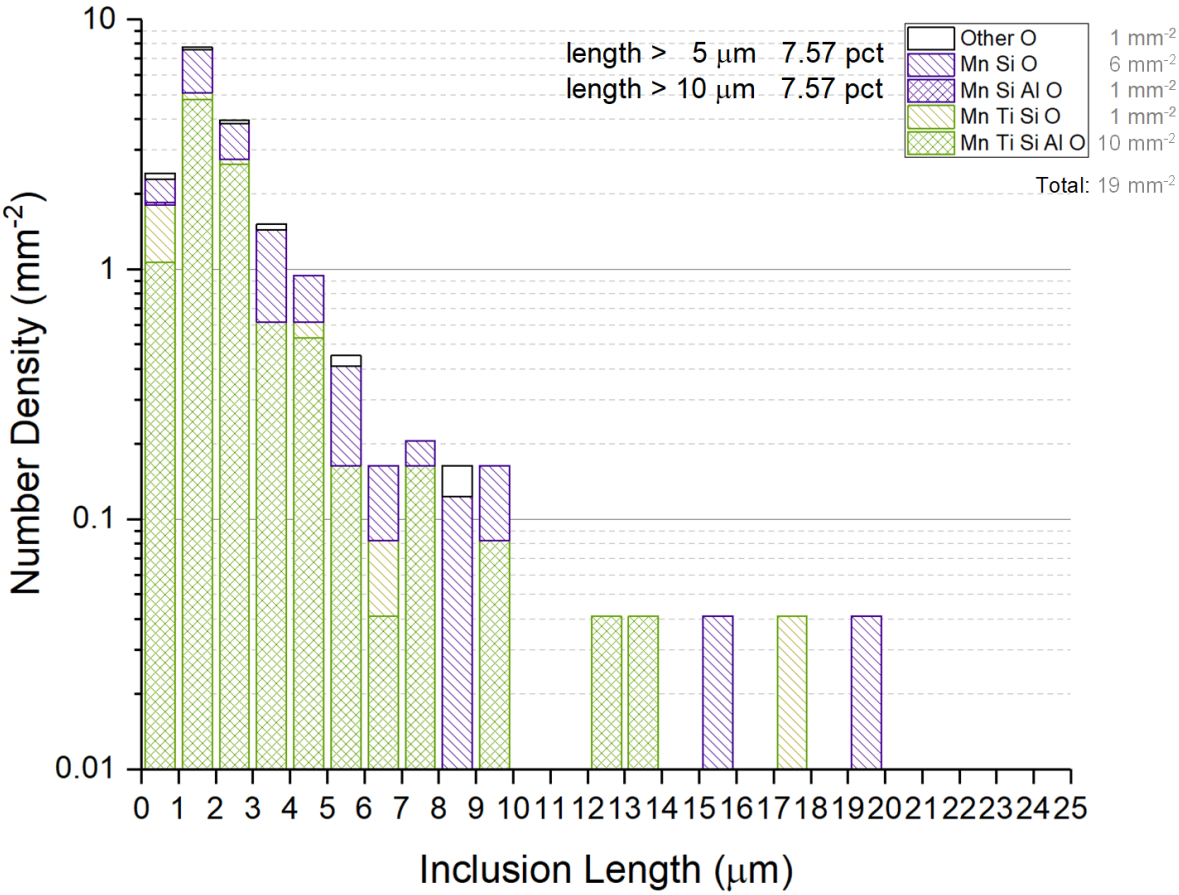
length > 5 μm 7.57 pct
length > 10 μm 7.57 pct
Other O 1 mm-2
Mn Si O 6 mm-2
Mn Si Al O 1 mm-2
Mn Ti Si O 1 mm-2
Mn Ti Si Al O 10 mm-2
Total: 19 mm-2
Number Density (mm-2)
10
1
0.1
0.01
0 1 2 3 4 5 6 7 8 9 10 11 12 13 14 15 16 17 18 19 20 21 22 23 24 25
Inclusion Length (μm)

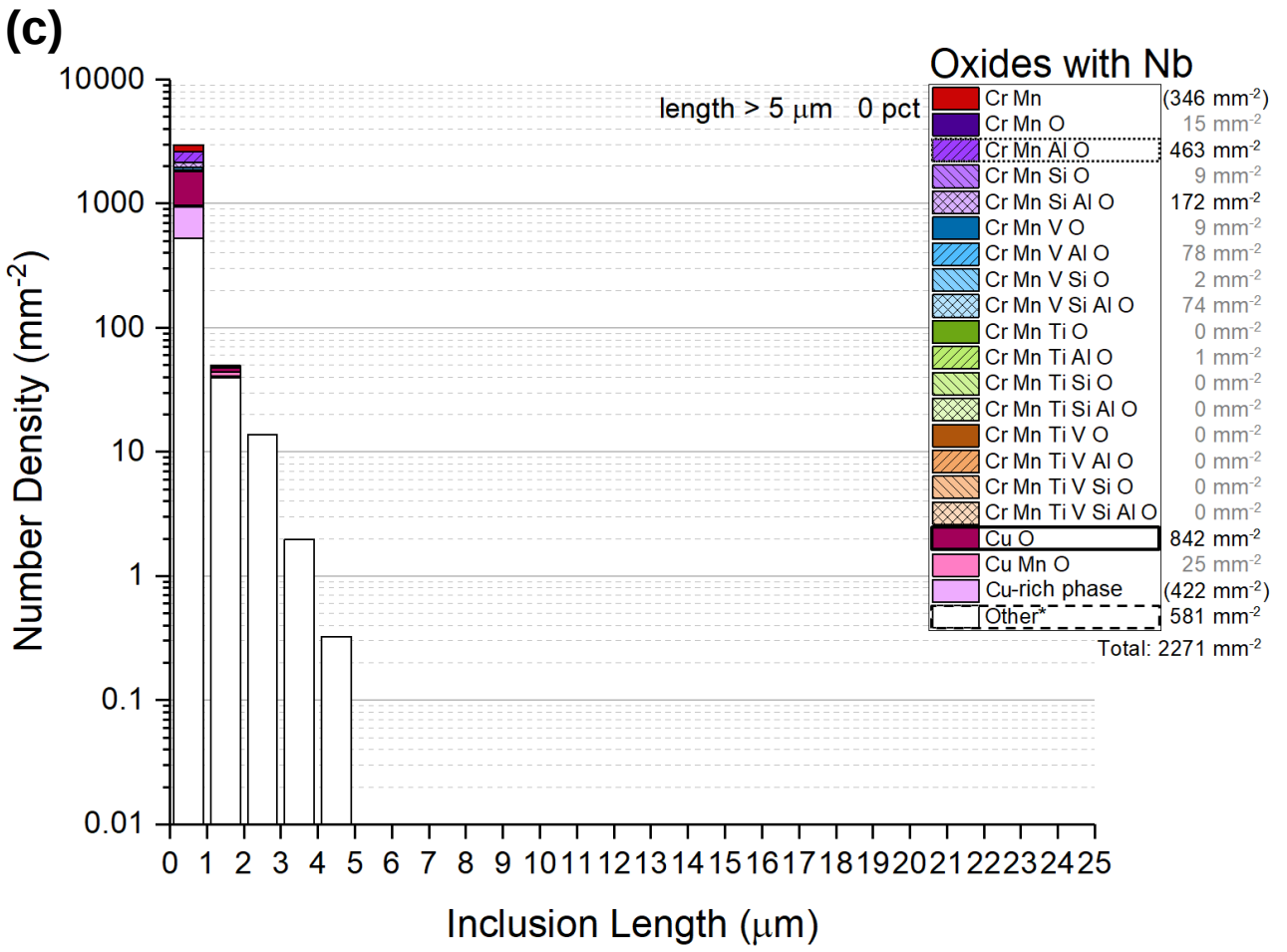
(c)
Oxides with Nb
length > 5 μm 0 pct
Cr Mn (346 mm-2)
Cr Mn O 15 mm-2
Cr Mn Al O 463 mm-2
Cr Mn Si O 9 mm-2
Cr Mn Si Al O 172 mm-2
Cr Mn V O 9 mm-2
Cr Mn V Al O 78 mm-2
Cr Mn V Si O 2 mm-2
Cr Mn V Si Al O 74 mm-2
Cr Mn Ti O 0 mm-2
Cr Mn Ti Al O 1 mm-2
Cr Mn Ti Si O 0 mm-2
Cr Mn Ti Si Al O 0 mm-2
Cr Mn Ti V O 0 mm-2
Cr Mn Ti V Al O 0 mm-2
Cr Mn Ti V Si O 0 mm-2
Cr Mn Ti V Si Al O 0 mm-2
Cu O 842 mm-2
Cu Mn O 25 mm-2
Cu-rich phase (422 mm-2)
Other* 581 mm-2
Total: 2271 mm-2
Number Density (mm-2)
10000
1000
100
10
1
0.1
0.01
0 1 2 3 4 5 6 7 8 9 10 11 12 13 14 15 16 17 18 19 20 21 22 23 24 25
Inclusion Length (μm)

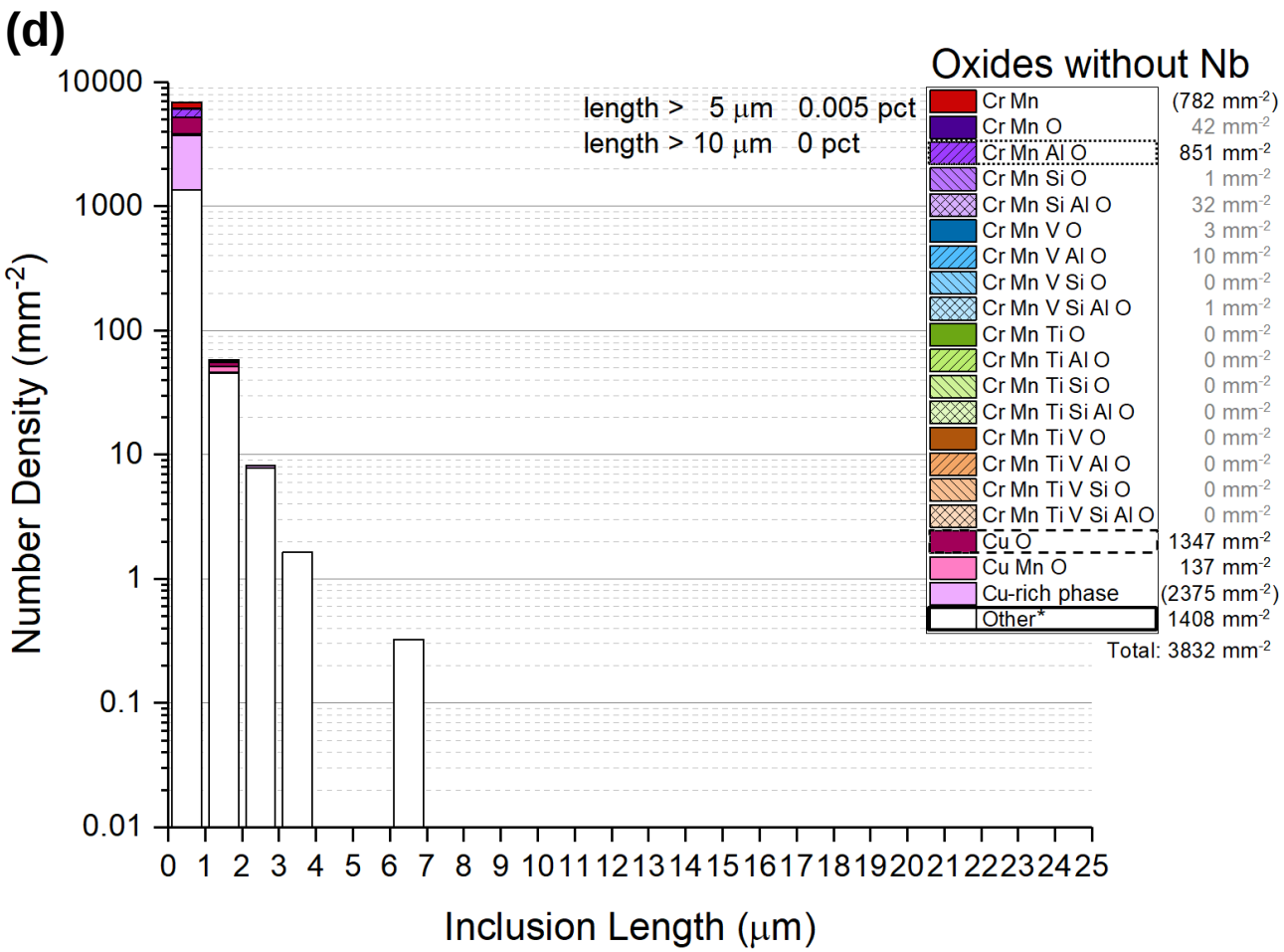
(d)
Oxides without Nb
length > 5 μm 0.005 pct
length > 10 μm 0 pct
Cr Mn (782 mm-2)
Cr Mn O 42 mm-2
Cr Mn Al O 851 mm-2
Cr Mn Si O 1 mm-2
Cr Mn Si Al O 32 mm-2
Cr Mn V O 3 mm-2
Cr Mn V Al O 10 mm-2
Cr Mn V Si O 0 mm-2
Cr Mn V Si Al O 1 mm-2
Cr Mn Ti O 0 mm-2
Cr Mn Ti Al O 0 mm-2
Cr Mn Ti Si O 0 mm-2
Cr Mn Ti Si Al O 0 mm-2
Cr Mn Ti V O 0 mm-2
Cr Mn Ti V Al O 0 mm-2
Cr Mn Ti V Si O 0 mm-2
Cr Mn Ti V Si Al O 0 mm-2
Cu O 1347 mm-2
Cu Mn O 137 mm-2
Cu-rich phase (2375 mm-2)
Other* 1408 mm-2
Total: 3832 mm-2
Number Density (mm-2)
10000
1000
100
10
1
0.1
0.01
0 1 2 3 4 5 6 7 8 9 10 11 12 13 14 15 16 17 18 19 20 21 22 23 24 25
Inclusion Length (μm)

(e)

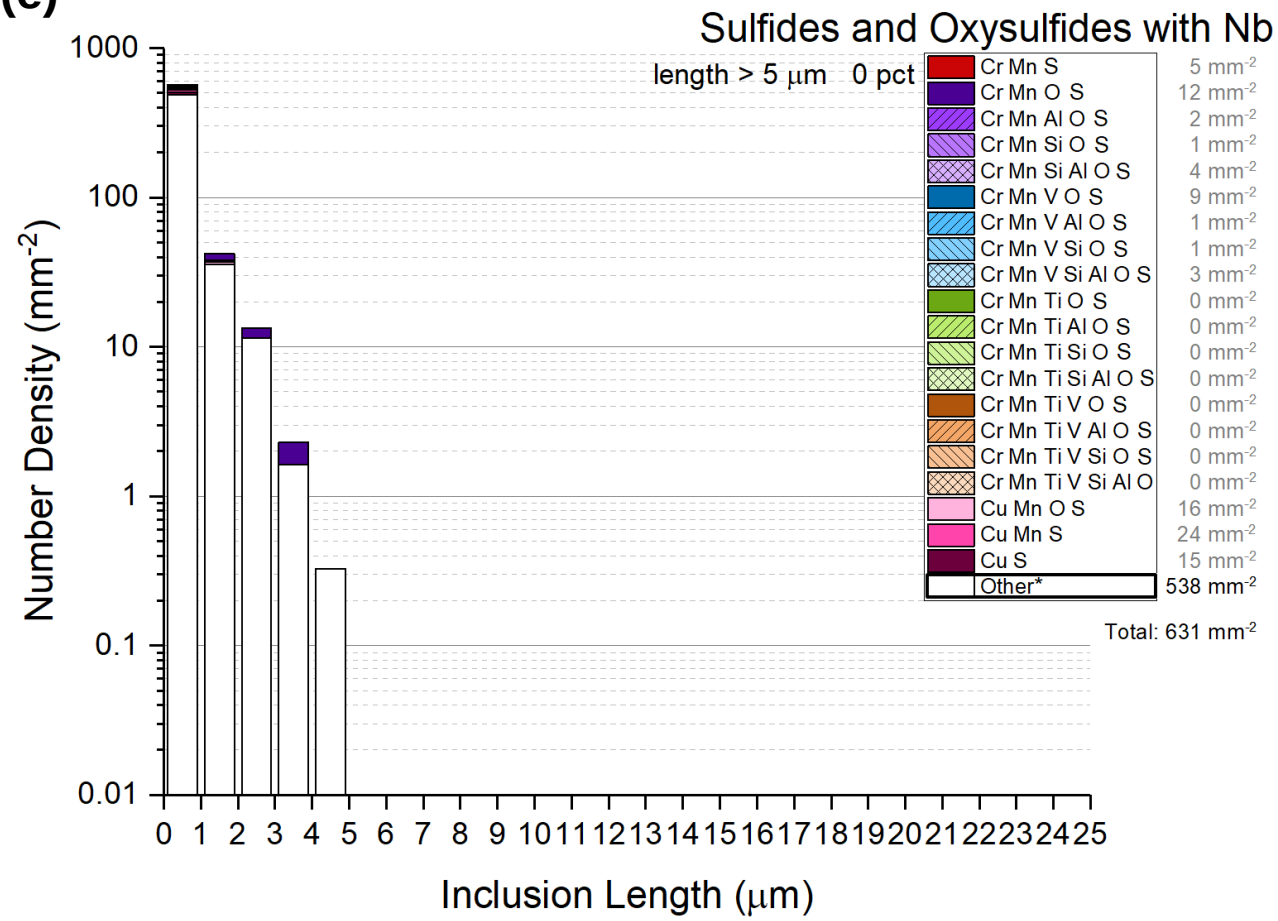
Sulfides and Oxysulfides with Nb
length > 5 μm 0 pct
Cr Mn S 5 mm-2
Cr Mn O S 12 mm-2
Cr Mn Al O S 2 mm-2
Cr Mn Si O S 1 mm-2
Cr Mn Si Al O S 4 mm-2
Cr Mn V O S 9 mm-2
Cr Mn V Al O S 1 mm-2
Cr Mn V Si O S 1 mm-2
Cr Mn V Si Al O S 3 mm-2
Cr Mn Ti O S 0 mm-2
Cr Mn Ti Al O S 0 mm-2
Cr Mn Ti Si O S 0 mm-2
Cr Mn Ti Si Al O S 0 mm-2
Cr Mn Ti V O S 0 mm-2
Cr Mn Ti V Al O S 0 mm-2
Cr Mn Ti V Si O S 0 mm-2
Cr Mn Ti V Si Al O 0 mm-2
Cu Mn O S 16 mm-2
Cu Mn S 24 mm-2
Cu S 15 mm-2
Other* 538 mm-2
Total: 631 mm-2
Number Density (mm-2)
1000
100
10
1
0.1
0.01
0 1 2 3 4 5 6 7 8 9 10 11 12 13 14 15 16 17 18 19 20 21 22 23 24 25
Inclusion Length (μm)

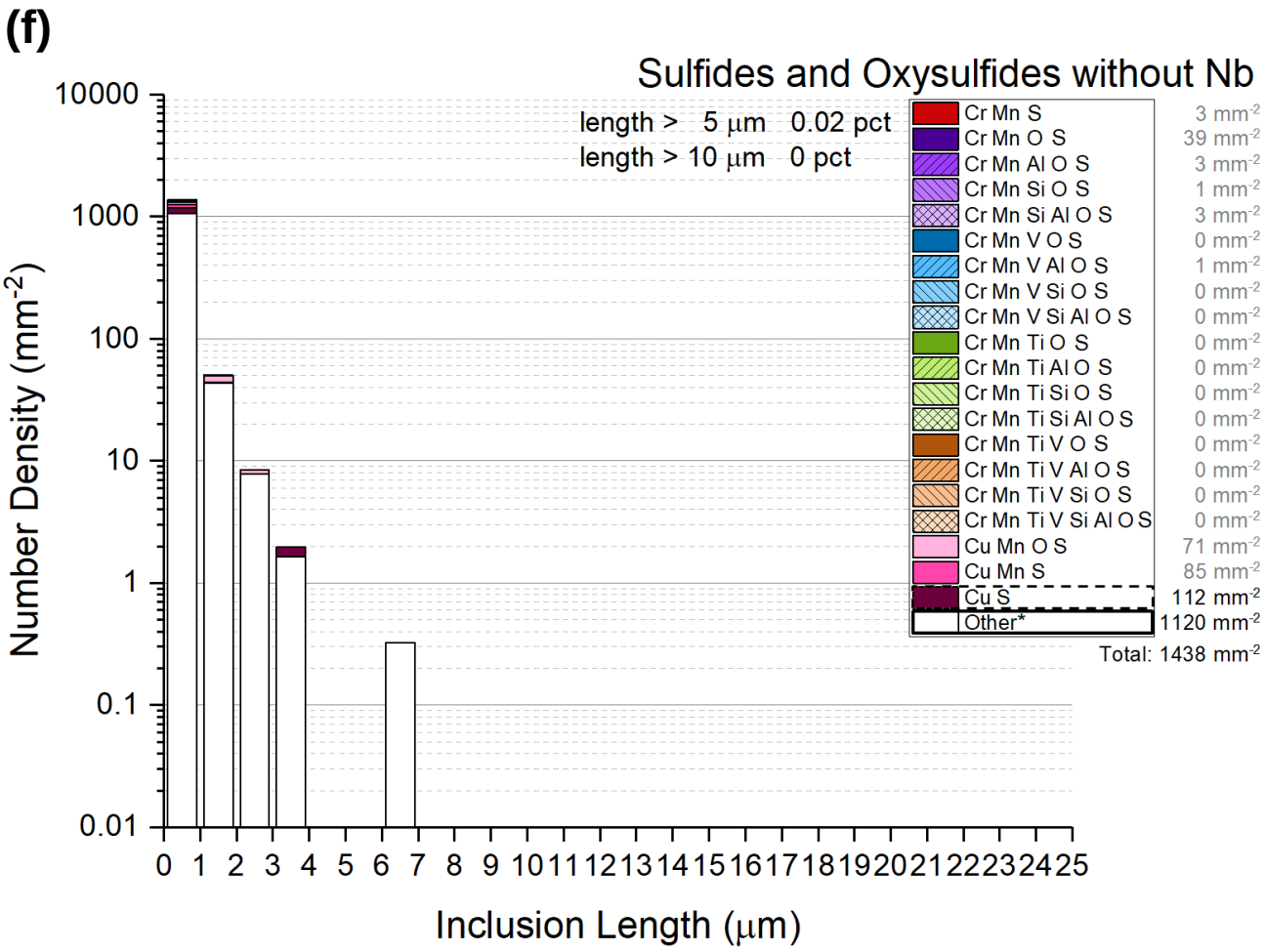

Fig. S-2 – Histograms of number density of non-metallic inclusions for the 17-4PH stainless steel: (*a*) feedstock; (*b*) VIGA powder < 150 µm; and (*c*), (*d*), (*e*) and (*f*) HIP´d 25 to 45 µm samples. See Fig. S-1 caption for notations. *Other inclusions having Cr levels less than the matrix value of 15.78 wt pct, they are mostly Al-rich.

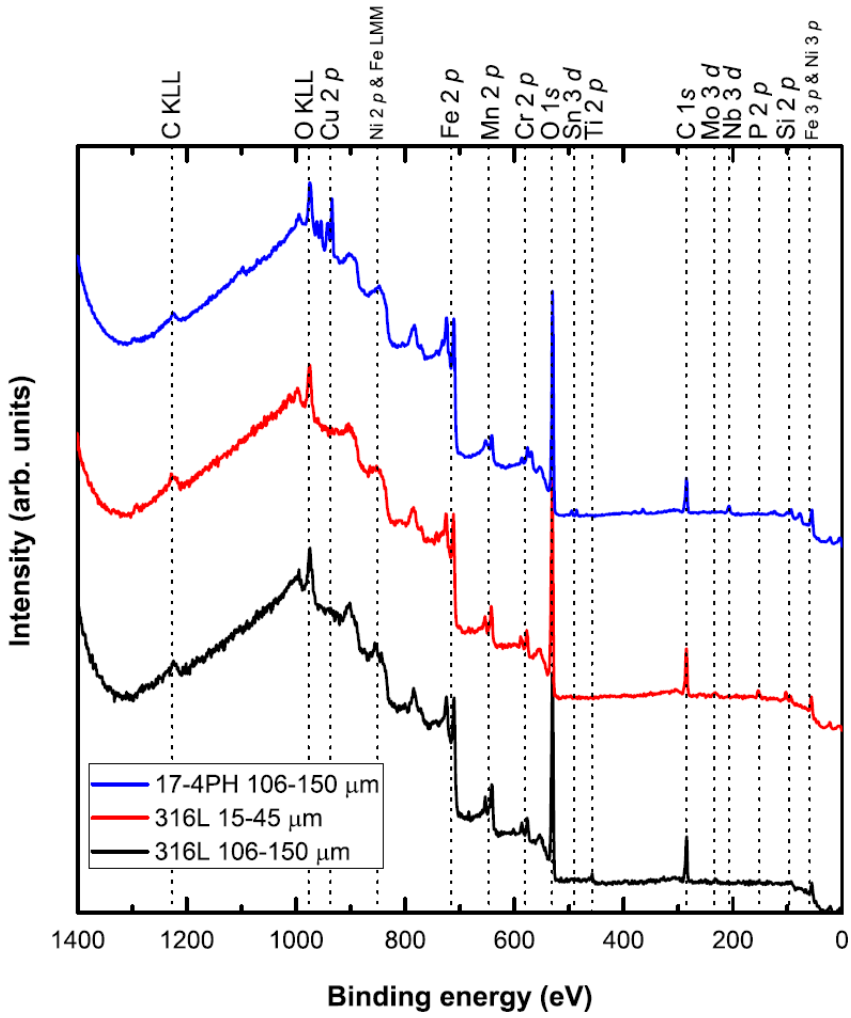

Fig. S-3 – Survey spectra acquired in the as-received condition from the three powders. The dotted lines indicate the approximate peak positions of the elements observed.

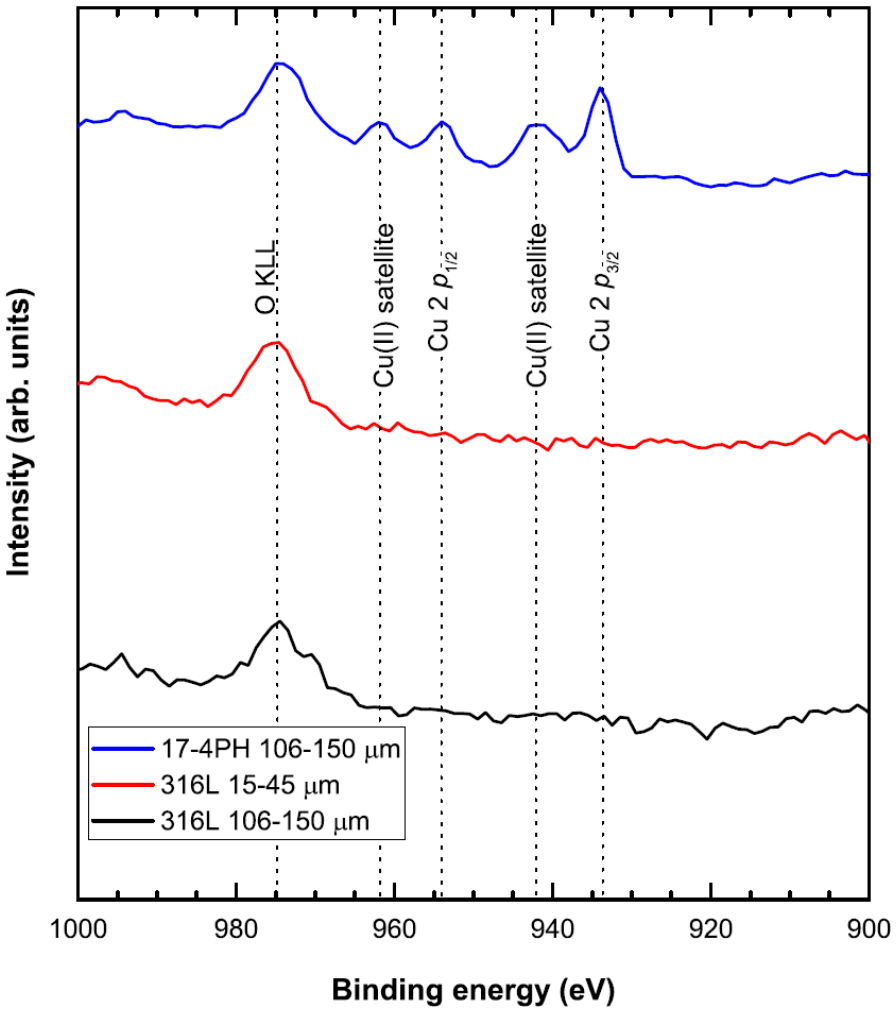

Fig. S-4 – The Cu *2p* and O KLL region of the spectra acquired in the as-received condition from the three powders, clearly illustrating that Cu was only detected from the surface of 17-4PH 106 to 150 μm.

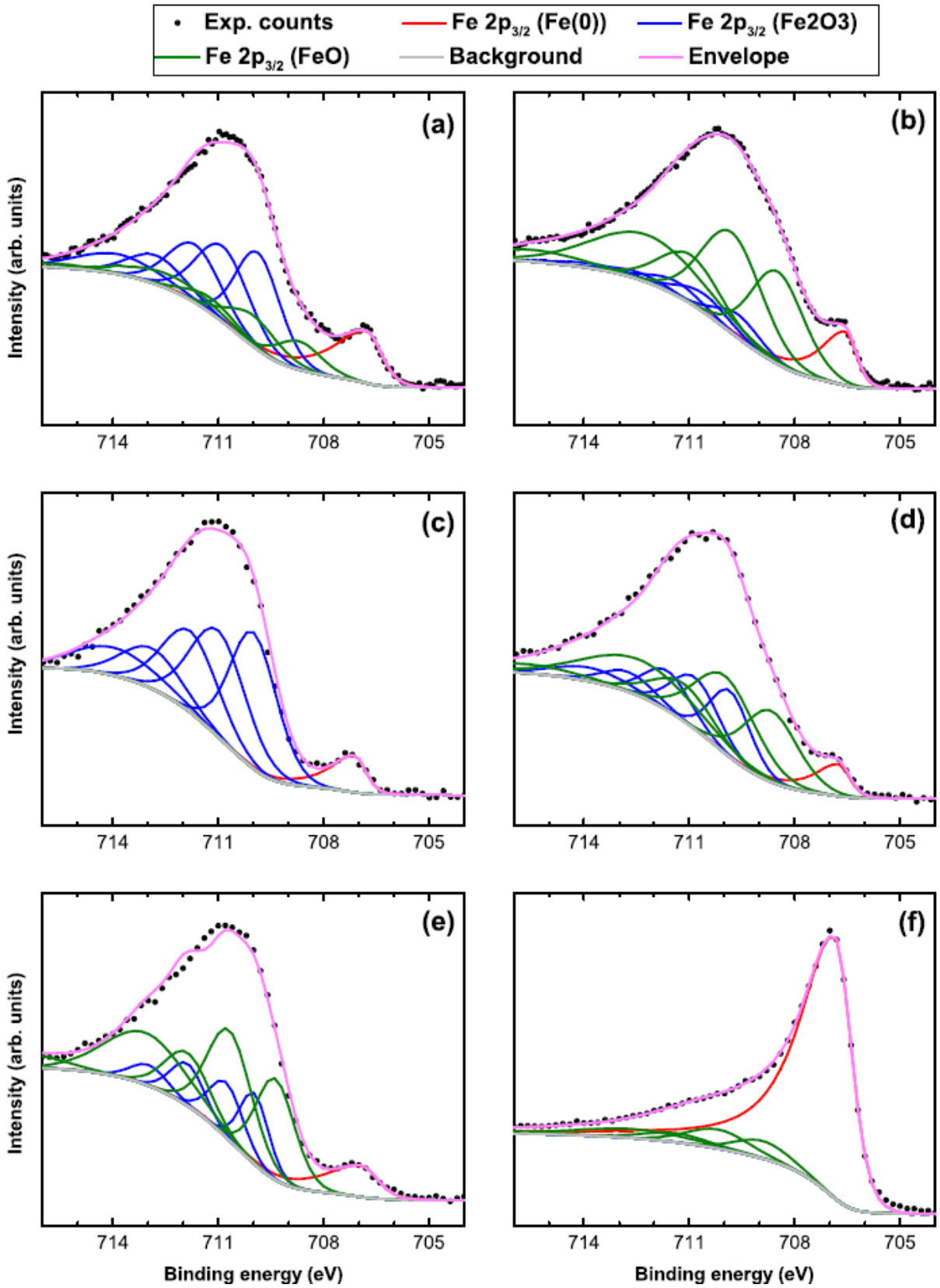

Fig. S-5 – Fe 2$p_{3/2}$ spectra acquired from the three powders: 316L 105 to 160 µm (*a*) as-received and (*b*) after sputtering; 316L 15 to 45 µm (*c*) as-received and (*d*) after sputtering; 17-4PH 106 to 150 µm (*e*) as-received and (*f*) after sputtering. Contributions from metallic Fe(0), FeO and Fe_2O_3 are seen throughout, as detailed in Table XI.

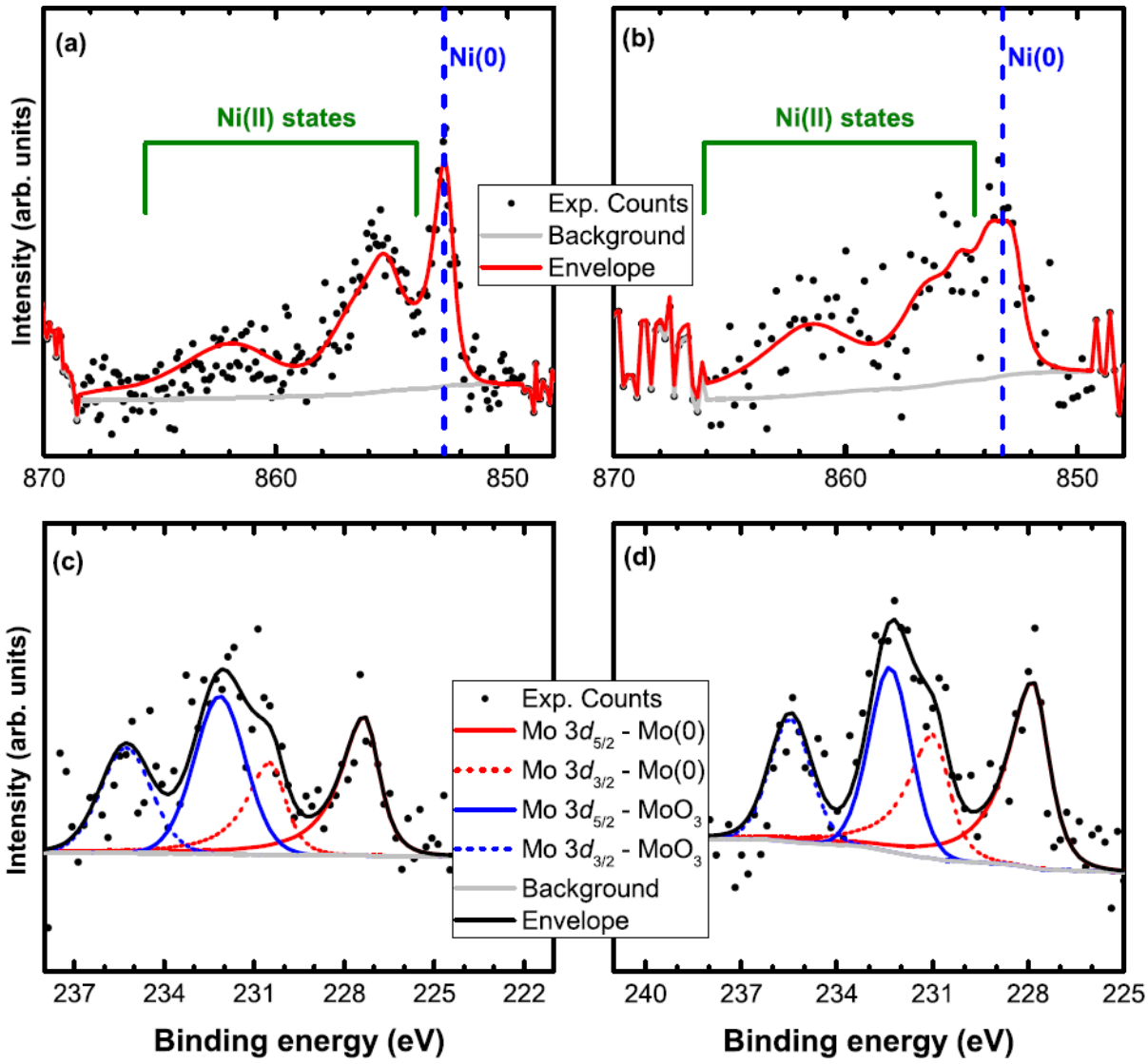

Fig. S-6 – High resolution core level spectra examining the Ni 2*p* region (*a*) and (*b*); and the Mo 3*d* region (*c*) and (*d*) for the presence of surface oxides. Both as-received 316L 106 to 150 µm (*a*) and (*c*); and the 316L 15 to 45 µm (*b*) and (*d*) presented evidence of Ni and Mo oxides near the surface. 17-4PH and did not have Ni or Mo in sufficient quantity near the surface to examine this effect.

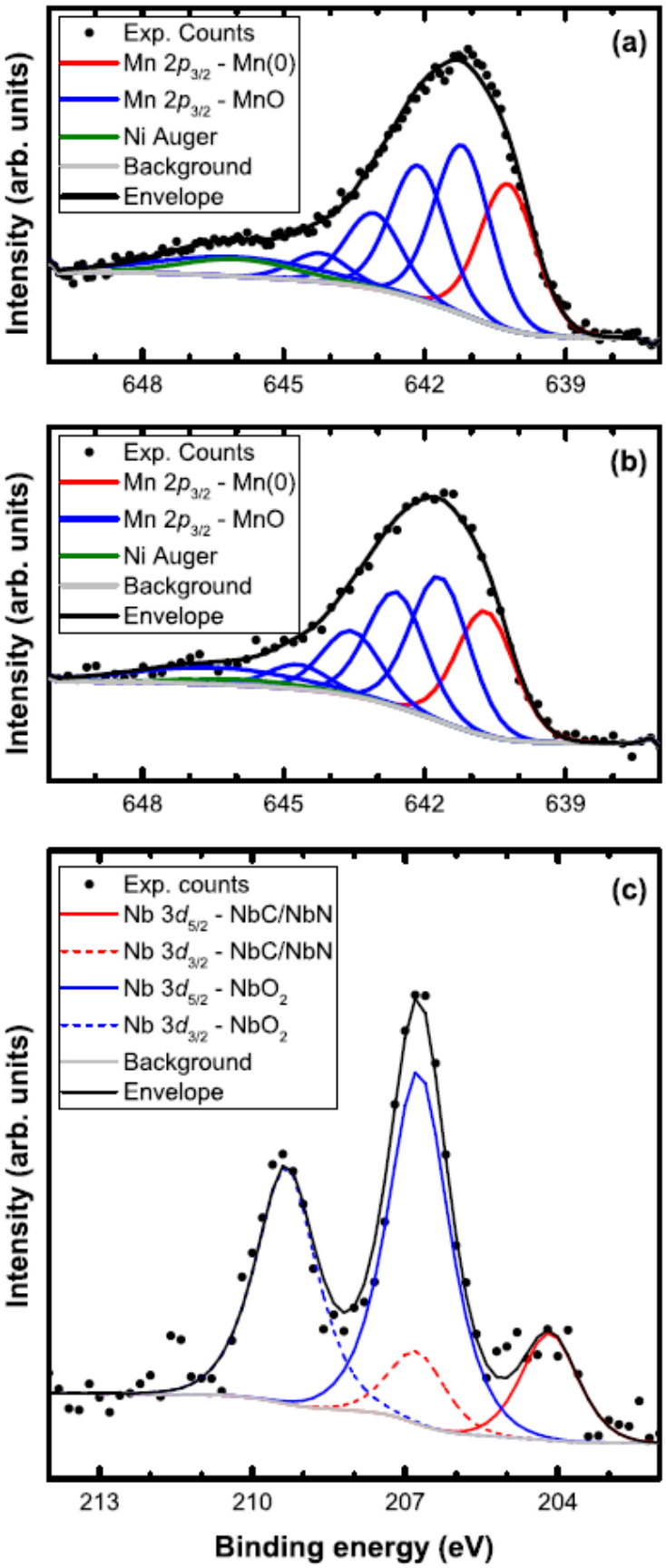

Fig. S-7 – Mn $2p_{3/2}$ spectra from (*a*) the 316L 106 to 150 µm powder and (*b*) the 316L 15 to 45 µm powder, showing the existence of MnO near the surface. Panel (*c*) shows the Nb 3*d* spectrum from the 17-4PH powder, with contributions from oxides and carbides and/or nitrides.

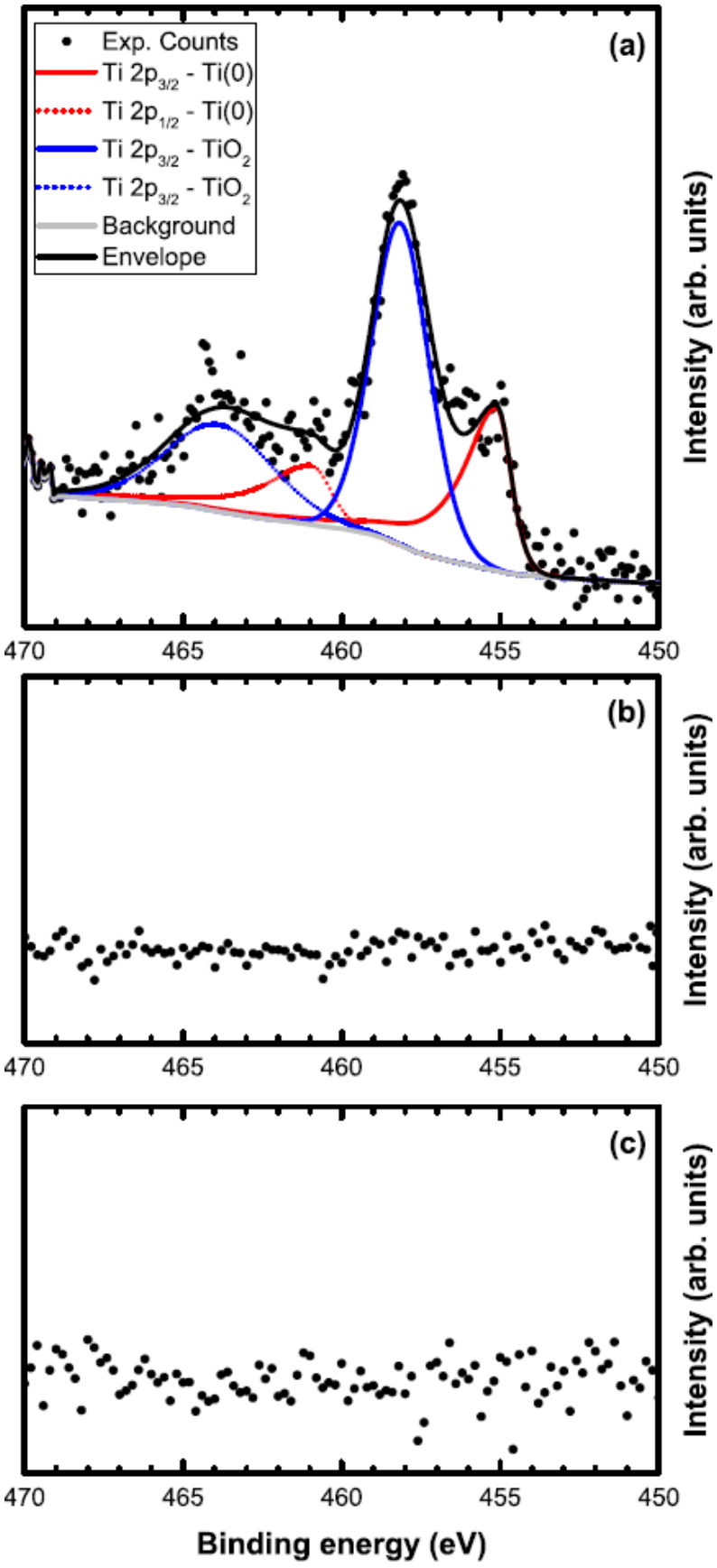

Fig. S-8 – Ti 2*p* spectra from (*a*) the 316L 106 to 150 µm powder, (*b*) the 316L 15 to 45 µm powder, and (*c*) the 17-4PH powder. Ti was only observed on the 316L 106 to 150 µm powder, with contributions from both metallic and oxidized Ti.

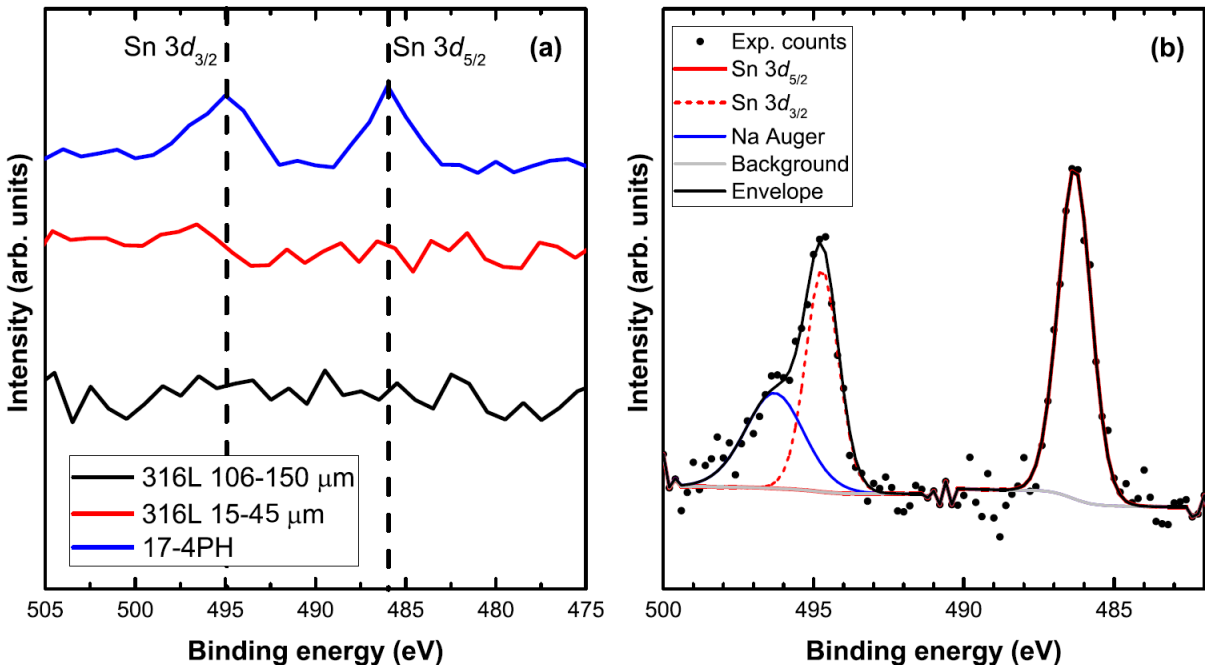

Fig. S-9 – (*a*) The Sn 3*d* region extracted from the survey spectra acquired from each of the three steel powders, showing that Sn was only detected in 17-4PH and (*b*) The high-resolution Sn 3*d* region from 17-4PH, showing the existence of Sn oxides on the surface.

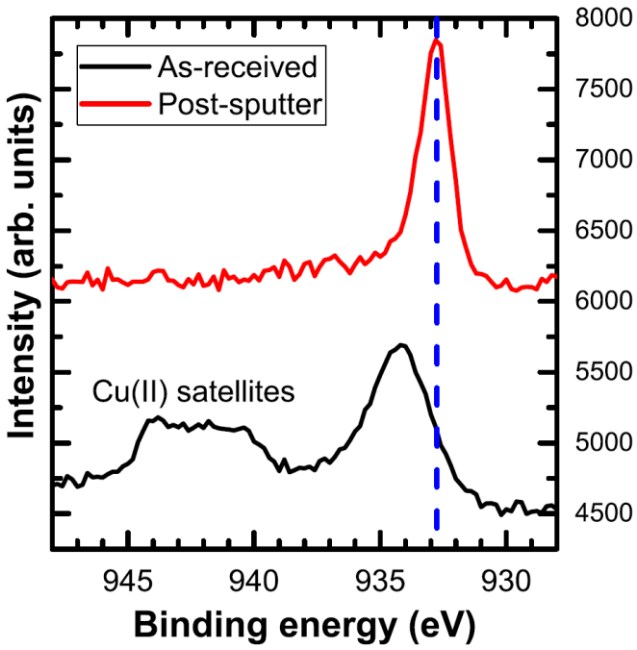

Fig. S-10 – The Cu 2$p_{3/2}$ region acquired from the 17-4PH powder in the as-received condition and after Ar^+ sputtering. The initial spectrum is dominated by Cu(II) components, but these are removed to reveal a Cu_2O layer and underlying metallic Cu. The blue dashed line indicates the binding energy of the main Cu 2$p_{3/2}$ component after sputtering, highlighting the downward energy shift of the envelope due to the removal of Cu(II) species.

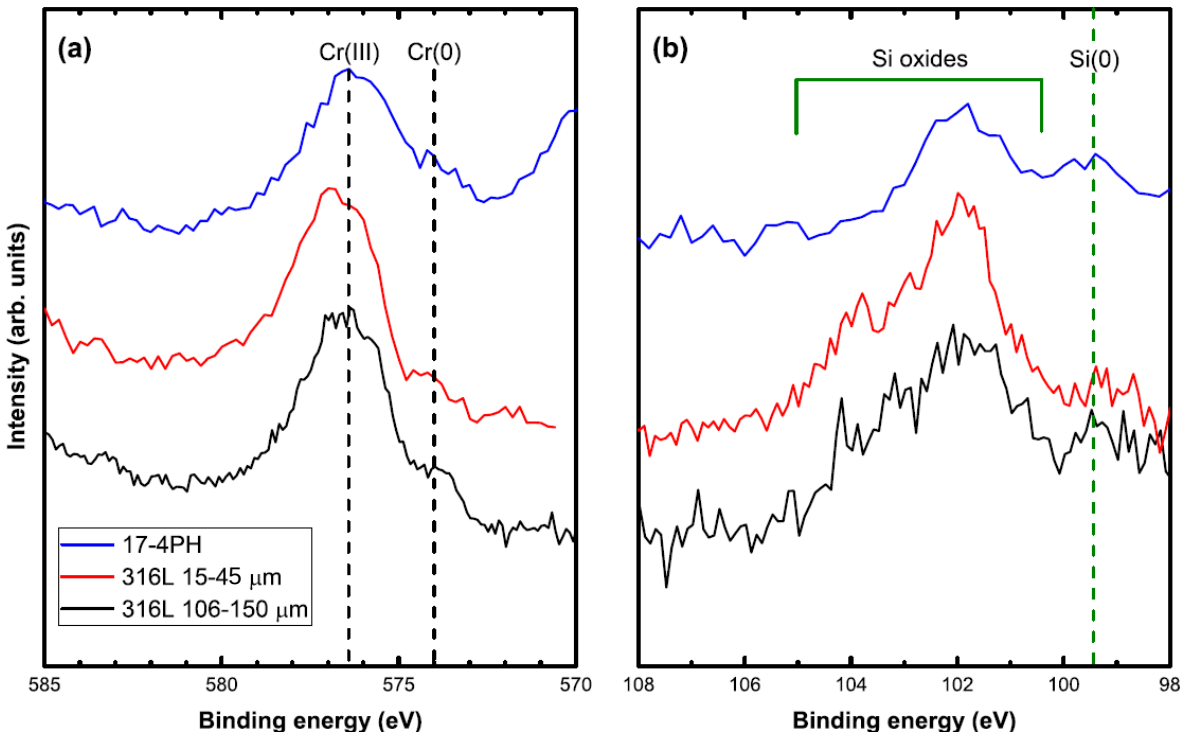

Fig. S-11 – (*a*) The Cr 2$p_{3/2}$ spectra acquired from the three powders in the as-received condition, showing the presence of both Cr(0) and Cr(III) species and (*b*) The Si 2*p* spectra acquired from each powder in the as-received condition, dominated by Si oxides but also showing a small contribution from Si(0).

Grain Size in the HIP'd 316L Steel

Grain size distributions (determined as equivalent grain diameter as the grains are approximately equiaxed) are plotted in supplementary Fig. S-12 and the corresponding average and standard deviation are also given in supplementary Fig. S-12. It can be seen that the as-atomized conditions exhibit much finer grain size microstructures compared to their HIP'd products, confirming grain growth during the HIPping and heat treatment process. The average and standard deviation grain size values in the AMGA HIP'd 316L < 150 μm were somewhat coarser (23.1 ± 21.6 μm) than those of the VIGA HIP'd 316L 106 to 150 μm (17.3 ± 15.4 μm). The AMGA HIP'd 316L < 150 μm sample would be expected to give a finer grain structure given the number density of non-metallic inclusions of the HIP's samples, but this is the opposite trend to that shown here. It is, however, of interest to note that Ti was partly retained in the VIGA HIP'd 316L 106 to 150 μm sample (0.05 wt pct), compared to the AMGA HIP'd 316L < 150 μm sample (< 0.005 wt pct). Grain refinement would then result from the presence of strong grain boundary pinning centers, e.g. Ti-rich carbonitrides, as some grain boundary pinning from precipitates has been observed in both HIP'd samples (Figures 10 and 11). Furthermore, a bimodal grain size is seen for the HIP'd 316L < 150 μm (air melted) material with 0.085 area fraction of 130 - 140 μm sized grains.

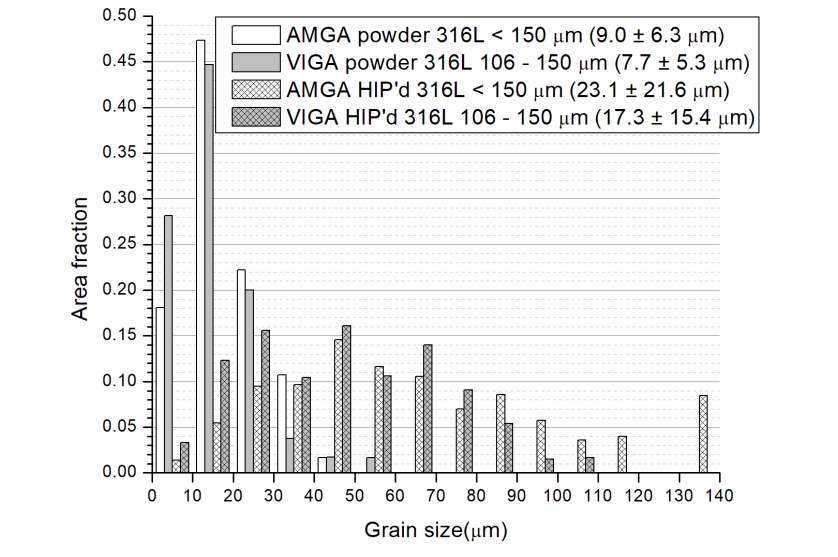

Fig. S-12 – Grain size distributions as measured by equivalent diameter in powders and after the HIPping and heat treatment process.
Reprinted with permission from Reference 17 copyright 2018, http://worldpm2018.medmeeting.org/Content/45181

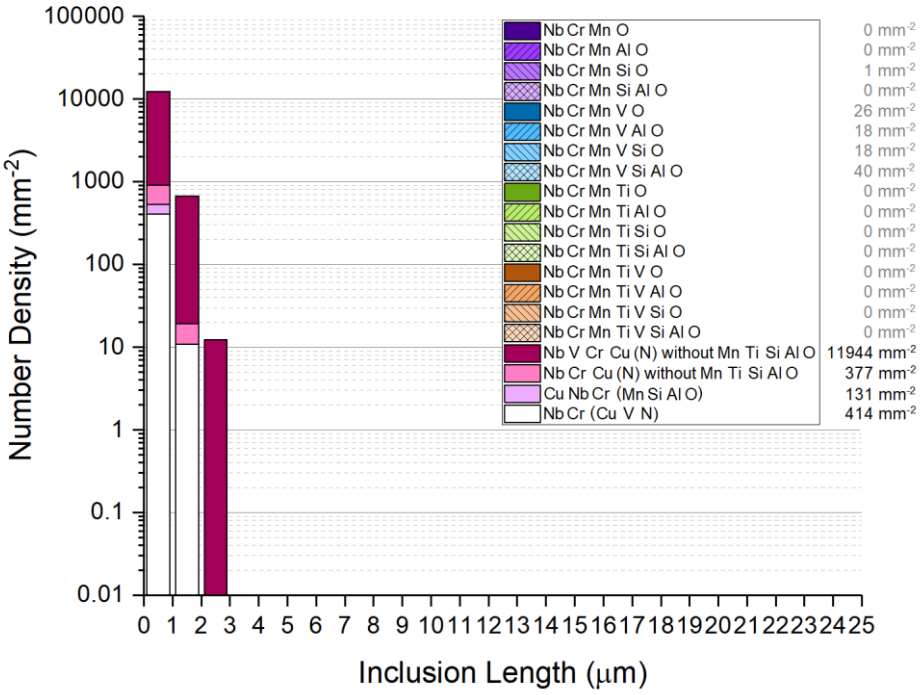

Fig. S-13 **–** Histograms of the number density of the white contrast phase in BSEI for the HIP'd 17 - 4PH 25 to 45 μm sample. Elements in parenthesis indicate that can sometimes be present or not.